Land tessellation effects in mapping agricultural areas by remote sensing at field level

DOI:10.1080/01431161.2019.1601287

Land Tessellation Effects in Mapping Agricultural Areas by Remote Sensing at Field Level

Borgogno Mondino, E; Corvino, G

Department of Agricultural, Forest and Food Sciences, University of Turin,

Largo Braccini 2, 10095, Grugliasco (TO), Italy

Corresponding author e-mail address: enrico.borgogno@unito.it

Land Tessellation Effects in Mapping Agricultural Areas by Remote Sensing at Field Level

While mapping agricultural areas by remote sensing it is quite common to operate at cadastral parcel level. Unfortunately this land tessellation is merely administrative: a single parcel can, in fact, be made of differently managed parts whose spectral properties can be significantly different, being often different their content. In this situation, approaches that aggregate spectral signals of pixels belonging to the same parcel to investigate their average behavior, can generate misleading results. In this work we evaluated how different field tessellation schemes can condition the interpretation of the spectral behavior of crops with special concern on time series of *NDVI* (Normalized Difference Vegetation Index) and *NDWI* (Normalized Difference Water Index) spectral indices, assumed as proxies of plant vigour and crop/soil water content, respectively. The study relies on Sentinel 2 and Landsat 8 data imaging a rice cultivated area sited in Piemonte (NW Italy). Two reference land tessellation geometries were taken into account: a) the local cadastral map (purely administrative land division criterion); b) a map obtained by image segmentation of the NDVI time series (purely spectral land division criterion). After signal aggregation some statistics were therefore computed to test differences both in time (within the same parcel along its temporal profile), and in space (within the same image at different positions at the same time). Results, obtained exploring the rice growing season 2016, showed that: a) in 23% (70% at 1 sigma) and 27 % (70 % at 1 sigma) of segments (respectively for NDVI and NDWI) spectral differences, averagely along the year, are significant, possibly leading to wrong interpretation of occurring dynamics in the area; b) in rice cultivated fields, spectral differences suffer from seasonality with a higher incidence in Spring, when rice agronomic phases are more dynamic and, in the meantime, critical for management.

Keywords: Spectral Indices; Image Time Series; Image Segmentation; Cadastral Parcels, Crop Monitoring

1: Introduction

Nowadays remote sensing techniques are widely used in agricultural applications due to the high availability of free pre-processed datasets, suggesting the implementation and supplying of services (possibly web-based) for crop monitoring tending to a better agronomic management by farmers and a more rigorous control of practices by institutional administrations (Hatfiel et al.,2008; Karantzalos et al., 2015; Kliment et al., 2014; Tey & Brindal, 2012). Nevertheless the adoption of remotely sensed images time series has proved to improve accuracy of classification of crops and surfaces during seasons (McNairn et al., 2009). While discussing about services for crop monitoring, it can be observed that, cadastral maps play an important role since, they are often used to aggregate spectral signal, thus assuming that no sub-parcel differentiated field management is possible (Erden & Öztürk, 2015; Erden & Töreyen, 2015; Zelaya et al., 2016); in these situations deductions from remotely sensed data can be highly misleading. Crops, in general, are observed at parcel level by averaging the spectral behavior of contained pixels, mostly synthesized by spectral indices as NDVI, SAVI (Soil Adjusted Vegetation Index), EVI (Enhanced Vegetation Index) etc. intended as predictors of some agronomic parameters (Hively et al., 2009; Huang et al., 2004; O' Connell et al., 2014; Zerbato et al., 2016).

Unfortunately, especially in the Italian agricultural landscape, the favourable situation where a single cadastral parcel is homogeneously managed, is often missing. The high fragmentation of territory and the national slow process of cadastral maps updating are majorly responsible of this fact. In many cases sub-parcel field division simply results in a time shift of farming operations determined by a not contemporary seeding of the same crop. In other more critical cases, it can be related to different crops that were planted in the different parts of the same parcel. Whatever is the condition, signal aggregation at parcel level (in general obtained by averaging spectral signal of the included pixels) determines a not controllable error that generate unreliable deductions concerning crop properties.

This critical feature of Italian (and not only) agricultural landscape is at the basis of the EU regulation no. 809/2014 that binds payment claims related to CAP (Common Agricultural Policy) to an electronic format, based on GIS (Geographic Information System): the "*geo-spatial aided application form* (GSAAF)". GSAAF is intended to limit errors by beneficiaries when declaring their agricultural areas, making administrative cross-checks more efficient. In addition, more accurate spatial information provided by GSAAF will provide more reliable data to monitor and evaluate agronomic practices, since the effective spatial distribution and extension of crops within, or over, cadastral parcels will be considered and declared by applicants. This is a new trend in respect of the current one where contributions are given with reference to the whole cadastral parcel. In Italy, GSAAF is expected to be based on aerial orthoimages supplied by National (AGEA) and Regional (ARPEA in Piemonte) agencies for payments in agriculture.

A rice cultivation devoted area was assumed as reference for this work since rice cultivation is mostly extensive and, in the Italian agricultural context, it appears as the most homogeneously managed. Consequently, if significant differences can be observed in this situation, more reasonably they could be found monitoring other crops. Moreover, rice is the most common staple food and it represents a grounded base for food security for about 3 billion people on Earth, especially in low- and lower-middle income countries (Maclean et al., 2002) It is cultivated under a wide range of management conditions: highly mechanised, irrigated, single summer cropping (i.e. Italy, Japan, the U.S., Australia, Brazil); rainfed rice systems across Latin America, sub-Saharan Africa, and South and South-East Asia (Boschetti et al., 2014). In Europe, Italy is the first rice producer having about $2.2 \cdot 10^5$ ha of cultivated areas and a production of $1.4 \cdot 10^6$ $t \cdot y^{-1}$ corresponding to the 52% of the rice devoted areas and 50% rice production in Europe, respectively (http://www.enterisi.it). Due to its flooded condition, rice is one of the main consumers of world fresh water resources (Tuong & Bouman, 2003), making desirable an efficient management.

The present work is part of a research project solicited by the Agriculture Department of the Piemonte Region Administration, that asked about an evaluation of effects that a different land tessellation scheme could generate while working with Normalized Difference Vegetation Index, NDVI (Rouse et al., 1974) and Normalized Difference Water Index, NDWI (McFeeters, 1996) time series. In particular Regional administrators were interested in monitoring the rice flooding phase at sub-parcel level to understand where and when water releases occur and how farmers use water. This is an important issue to deal with since water demand in rice-cultivation generates a high pressure on water resource especially during the rice-fields flooding step.

Rice crop monitoring by spectral indices time series is known to be effective in describing main farming operations along the year: a) pre-seeding fields submersion , b) plant emersion from water, c) pre-harvest ripening. NDVI and NDWI were selected as reference indices being widely used to monitor crop phenology and crop irrigation dynamics. In particular, NDVI proved to be able to monitor plants vigour; NDWI to describe crop water status.

A composite image time series from Sentinel 2 and Landsat 8 datasets were used for this purpose. According to the above mentioned tessellation schemes, differences affecting spectral indices temporal profiles were tested both in time (within the same parcel along its temporal profile), and in space (within the same image at different positions at the same time).

Authors are conscious that results obtainable for a rice cultivated area cannot be completely generalized for whatever agricultural context. Nevertheless, results from this situation are expected to be optimistic in respect of any other crop, since rice fields, here, are known to be homogeneously and extensively managed, reasonably limiting local differences, that, for other crops will be certainly higher.

2: Materials and Methods

2.1: Test Area

The study area (about 8700 ha) is located in the Piemonte Region (NW Italy, Figure 1). From the agricultural point of view, it is mainly devoted to rice cultivation; ISTAT (Italian National Institute for Statistics) estimated that in 2016, rice crops took 116325 ha with a production of 499273 tons within the whole Vercelli province where this area is sited (ISTAT, 2018).

[FIGURE 1]

2.2: Available data

Twenty-two optical satellite images, covering the 2016 rice growing season, were used for this work: twelve ESA (*European Space Agency*) Sentinel-2 Level 2A images (hereinafter called S2) were obtained from the Copernicus Scientific Data Hub (*https://scihub.copernicus.eu/*); ten NASA (*National Aeronautics and Space Administration*) Landsat-8 images C1 Level 2 (hereinafter called L8) were obtained from the Earth Explorer (*https://earthexplorer.usgs.gov/*) archive of the USGS (US Geological Survey). Main technical features of both datasets are reported in Table 1.

[TABLE 1]

The above mentioned processing levels indicate that both the datasets were obtained as at-the-ground reflectance calibrated images. S2 and L8 images were jointly used to improve the temporal resolution of time series, especially during spring, when clouds often cover the area. L8 images were preventively oversampled to the same Ground Sample Distance, GSD, of S2 (10 m). Temporal distribution of satellite images is reported in Figure 2 showing that the joint use of both datasets was helpful to reduce the effect of cloud cover in the study area.

[FIGURE 2]

As far as S2 and L8 image integration is concerned, and specifically focusing on the joint use of NDVI and NDWI spectral indices, it has already been demonstrated that they are consistent enough to be aligned along the same time series (Barazzetti et al., 2016, Lessio et al., 2017; Munyati, 2017).

A vector cadastral map (1:2000 scale, WGS84 UTM 32 N reference frame) was also available for this work from the Piemonte Region Agricultural Department.

2.3: Data processing

Starting from the available at-the-ground reflectance calibrated images, the correspondent NDVI and NDWI spectral indices were computed for both L8 and S2 images according to eq.1 and 2.

$$NDVI = \frac{\rho_{NIR} - \rho_{RED}}{\rho_{NIR} + \rho_{RED}} \quad ; \quad NDWI = \frac{\rho_{GREEN} - \rho_{NIR}}{\rho_{GREEN} + \rho_{NIR}} \qquad (1, 2)$$

where ρ_{NIR}, ρ_{RED}, ρ_{GREEN} are the at-the-ground reflectances respectively for the Near Infrared, Red and Green bands, that are slightly different for the two datasets (Table 1).

Two different time series of NDVI/NDWI images were obtained by averaging the local spectral profiles, of neighbor pixels, according to different land tessellation schemes: the first based on cadastral parcels as defined by the available cadastral map; the second obtained by image segmentation of the original NDVI time series. Segmentation was operated by a region-growing based algorithm (Comaniciu & Meer, 2002) available in Orfeo ToolBox (OTB, v. 6.4.0). Image segmentation is known to detect homogeneous portions of land in terms of similar spectral properties. At this point it is worth to stress that spectral similarities of crops do not follow administrative boundaries. Consequently, segments can represent areas completely included in a single parcel (sub-parcels) or wider areas including portions of different adjacent parcels that behaves similarly. In this second case, the administrative geometric coherence (which part of segments does belong to a certain parcel?) can be easily recovered by intersection operations, involving cadastral parcels and segments vector layers, achieved by ordinary GIS tools. To give a description of the degree of sub-parcel potential fragmentation in the area we counted the number of segments that totally, or partially, fell into each cadastral parcel. The correspondent cumulative frequency distribution was therefore computed.

Since authors' hypothesis was that land portions of spectral homogeneity are different from cadastral parcels, expectation was that: a) segmented patches (objects) were more numerous than parcels; b) patches size was, generally, smaller. Consequently, some statistics concerning shape properties of both segmented polygons and cadastral parcels were computed by SAGA GIS software and compared. In particular patches area and *Shape Index* (*SI*, Forman & Godron, 1986) values (eq. 3) were compared computing the correspondent cumulative frequency distributions.

$$SI = \frac{P}{2\sqrt{\pi A}} \qquad (3)$$

where *P* is the polygon perimeter and *A* its area. SI represent circular objects when equal 1, square objects when around 1.128 and tends to increase for complex objects having highly moved borders (a long perimeter in respect of a limited area).

Successively, the following four time series of locally averaged spectral indices were obtained: NDVI and NDWI in respect of cadastral map (*NDVI(x,y,t)*^{c}, *NDWI(x,y,t)*^{c}); NDVI and NDWI in respect of segmentation result (*NDVI(x,y,t)*^{s}, *NDWI(x,y,t)*^{s}). Comparison was achieved at both temporal and spatial level.

Investigation at "spatial level" was achieved computing the local NDVI and NDWI *Mean Absolute Errors* (MAE, Willmott & Matsuura, 2005), obtaining two maps of MAE, hereinafter called $MAE(x,y)^{NDVI}$ and $MAE(x,y)^{NDWI}$ (eq. 4, 5).

$$MAE(x,y)^{NDVI} = \frac{\sum_{i=1}^{n}|NDVI(x,y,i)^s - NDVI(x,y,i)^c|}{n\_images} \qquad (4)$$

$$MAE(x,y)^{NDWI} = \frac{\sum_{i=1}^{n}|NDWI(x,y,i)^s - NDWI(x,y,i)^c|}{n\_images} \qquad (5)$$

where *n_images* is the total number of images (dates) belonging to the compared time series.

$MAE(x,y)^{NDVI}$ and $MAE(x,y)^{NDWI}$ were used to explore if differences were homogeneously distributed in the area.

Investigation "at time level" was, differently, performed by computing, for each explored date, the correspondent $MAE(t)^{NDVI/NDWI}$ from differences of the same time layer (eq. 6 and 7).

$$MAE(t)^{NDVI} = \frac{\sum_{i=1}^{c}\sum_{i=1}^{r}|NDVI(i,j,t)^s - NDVI(i,j,t)^c|}{n\_pixels} \qquad (6)$$

$$MAE(t)^{NDWI} = \frac{\sum_{i=1}^{c}\sum_{i=1}^{r}|NDWI(i,j,t)^s - NDWI(i,j,t)^c|}{n\_pixels} \qquad (7)$$

where *c* and *r* are, respectively, the number of columns and rows of the raster layer of differences at the single date, *NDVI/NDWI(x,y,t)* the local index value over the image at the date *t* and *n_pixels* the number of “good” image pixels (excluded cloudy or failed pixels).

This resulted into a time series made of 22 MAE(t) numerical values, each synthesizing the average difference over image at the single date.

Both MAE maps and temporal profiles were finally analysed looking for an interpretation key able to detect the main factors that, eventually, made an object-based approach more desirable than the one based on cadastral parcels.

3. Results and Discussions

Concerning segmentation of the original NDVI time series by OTB, the “mean-shift” algorithm was used with the following parameters: spatial radius = 5 pixels; range radius = 0.1; minimum region size = 25 pixels (i.e. 0.25 ha, assumed as the minimum mapping unit (MMU). Parameters properness was tested through some repeated tests. In figure 3 cadastre- and segmentation-based tessellation schemes are shown together with maps resulting from NDVI values averaged at field level (example area at April 2016).

[FIGURE 3]

In figure 4 the cumulative frequency distribution of segments per parcel (totally, or partially, contained) is reported to highlight the degree of sub-parcel divisions in the area.

[FIGURE 4] new addition

From a strictly geometrical point of view, the different type of landscape tessellation scheme (cadastre- and object- based) determined a significantly different number of patches: 4111 cadastral parcels showed an area greater or equal to 0.25 ha (consistent with the segmentation algorithm parameters); 6788 objects were obtained by segmentation (+ 65% in respect of cadastral parcels). Polygons area mean value (> 0.25 ha) passed from 1.20 ha (cadastre) to 0.80 ha (segmentation) with a reduction of 33%. *SI* mean value passed from 1.50 to 1.74 moving geometries from a more regular (squared) shape to a more irregular one. Cumulative distribution functions of both *Area* and *SI* values were computed and reported in figure 5.

[FIGURE 5]

Looking at the *Area* distribution (figure 5, left) it can be observed that: a) no significant changes occurred for smaller parcels (as expected) being, reasonably, always managed unitarily; they represent the 50% of the total, suggesting that, the proposed methodology will not affect this percentage of parcels; b) starting from parcels that were sized over 0.75 ha, the two compared distributions tended to differentiate much more, showing that, in terms of homogeneity of spectral response (NDVI, i.e. vigor), cadastral parcels are often managed differently (sub-parcel approach).

Looking at the distribution of *SI* (figure 5, right) it can be observed that in general, cadastral parcels show a more regular shape (tending to a squared geometry) as the highest percentage of polygons with lower *SI* demonstrate. Segmentation result was compared, by photointerpretation, with a false color composite RGB from the S2 dataset (R=b8, G=b4, B=b3; acquisition date: 21st July 2016), showing that the most of sub-parcel segments were related to the country roads and channels networks, whose traits are often included in the parcel, determining a significant variation of its average spectral response together with an obvious geometrical decomposition of the whole parcel. Some other sub-parcel segments, differently, were related to different local spectral responses of the same parcel, possibly indicating a different intra-parcel behavior of crop. The consequent question is therefore: is the average spectral response of the parcel homogeneously shifted from the expected value due to the inclusion of channels/roads? Or, possibly, is a differentiated management of parcels the responsible of sub-parcel spectral differences occurrences?

To answer this question some samples temporal profiles were extracted from the NDVI and NDWI averaged images and compared. In general, the spatial decomposition generated by segmentation within a parcel generated significantly different temporal profiles of spectral indices, indicating that, commonly in the area, a single large cadastral parcel cannot be considered unitary from the agronomic point of view. Differences between spectral index temporal profiles averaged over the whole parcel, and those averaged separately for the segments falling within the parcel can be interactively tested singularly. An example of these differences is given, for an example parcel, in figure 6, where NDVI (left) and NDWI (right) profiles averaged at segment level (black lines) are compared with those averaged at parcel level (red line). It can be easily noted that profile shapes are significantly different (sometime higher than 0.1 and 0.2 points for NDVI and NDWI, corresponding to a percentage difference of about 40% (0.1/0.25) and 100% (0.2/(-0.2)), respectively.

[FIGURE 6]

Moreover, sample profiles reported in figure 6 suggest a seasonality in differences: NDVI highest differences mainly affect the starting part of the growing season (beginning of March - end of June), indicating that crop proceeds on with different velocities at different times, especially during its germination and tillering phases. In the same way NDWI highest differences occur in April when water releases from the local Irrigation Consortium enter the fields to operate the pre-seeding submersion, suggesting a not homogeneous distribution of water at parcel level. Consequently, it can be said that segmentation improve crop behaviour interpretation, permitting a better management of fields (farmer's point of view) or a more punctual control of water releases (Consortium's point of view). A generalization of the reading key offered by figure 6 can be somehow achieved by aggregating measures of differences through the synthetic statistic parameters of equations 4-7.

Maps showing the spatial distribution of NDVI/NDWI MAE ($MAE(x,y)^{NDVI}$ and $MAE(x,y)^{NDWI}$) were obtained by averaging differences at pixel level along its temporal profile (eq. 4,5). A subset of the generated maps is reported in figure 6, where it can be observed that the mean MAE local value is spatially varying. Maps confirm that MAE values are higher for NDWI; they can be used to investigate, over the area, where the most critical situations are located. This is an important issue especially when monitoring water releases for control purposes from institutional players (like Consortium); moreover this represents a further demonstration that a parcel-based approach it is not enough to satisfyingly describe actual behaviors of crop/water dynamics.

[FIGURE 7]

At the moment authors are not able to give an interpretation key to robustly explain why some areas are more critical than others. The different behaviors of the various parts of the same parcel can rely on many motivations: different crop type, different treatments times, different terrain properties, position of fields in respect of the channel network, etc. An important issue to deal with when testing significance of differences, is the expected theoretical accuracy of NDVI/NDWI measures. Reference values for accuracy of NDVI/NDWI measures from satellite imagery can be found in literature (Borgogno-Mondino et al., 2016). For vegetated areas, they are told to be reasonably about 0.02 (1 sigma) - 0.04 (2 sigma) points of NDVI/NDWI. Consequently, only differences higher than these values have to be taken into account to demonstrate the impact of the different approaches in reading crop and water dynamics in the area.

To test this condition, the cumulative frequency distribution function was computed for both the above mentioned MAE maps and reported in figure 8 in respect of the number of segments.

[FIGURE 8]

From the graph, it can be noted that: about 77 % of segments, averagely along the year, have a NDVI value that, in respect of the correspondent cadastral parcel, is lower than 0.04 points, i.e. not significant; from these, ~ 30% is lower than 0.02. Similarly, about 73 % of segments, averagely along the year, show an NDWI value that, in respect of the correspondent cadastral parcel, is lower than 0.04 points, i.e. not significant; but, again, ~ 30% is lower than 0.02.

Conversely, in 23% (70% at 1 sigma) and 27 % (70 % at 1 sigma) of segments (respectively for NDVI and NDWI) spectral differences, averagely along the year, are significant, possibly leading to wrong interpretation of occurring dynamics in the area.

It is worth to remind that maps and statistics of figure 7 and 8, respectively, just point out average occurrences and values of spectral index differences along the year. Consequently, they cannot point out eventual criticalities related to a specific moment along the growing season.

Trying to give a preliminary answer to this question, seasonality of NDVI/NDWI MAE was explored computing the correspondent average profiles by eq. 6, 7. In figure 9, the average MAE profile is reported (gray line) together with maximum and minimum differences recorded at the single explored date. The average trend confirms what was locally observed in the sample parcel of figure 6. The comparison of the average MAE profile with those representing the maximum and minimum differences at the same time over the scene, demonstrates that differences can reach values higher and higher than the average one, making more desirable the adoption of segments in place of parcels to reduce the risk of misunderstanding of measures.

[FIGURE 9]

Focusing on the MAE average time profile ($MAE(t)^{NDVI/NDWI}$), it can be observed that maximum values were detected on the 19/04/2016 (start of growing season) and 21/05/2016 (during the typical first flooding step) for NDVI (about 0.07) and NDWI respectively (about 0.11), corresponding, in terms of farming operations, to flooding and plants development phases. Reported profiles show that, all along the year, average MAE is always higher than NDVI/NDWI reference value (1 sigma = 0.02), demonstrating that no measured difference is actually negligible; conversely, an approach based aggregating spectral signal at parcel level can lead to interpretation errors while monitoring crop and water dynamics in rice fields, especially in Spring, where differences appear to be higher.

4. Conclusions

The current period is showing an increasing demand and offer of services for agriculture based on the continuous monitoring of crops at regional level by remote sensing. Free archives of satellite imagery (both optical and radar) from main institutional suppliers (NASA/USGS and ESA), is accelerating the transfer of this type of technology to the operational compart. Scenarios for remote sensing adoption in agriculture are various, ranging from plant, to field up to region level, each defining its proper players and data. This work explore a criticality mainly related to the region level approaches, where applications are mainly devoted to management of wide areas where, in many cases, the minimum mapping unit to be investigated is assumed to be the cadastral parcel. Unfortunately this land tessellation is merely administrative: a single parcel can, in fact, be made of differently managed parts whose spectral properties can be significantly different, being often different their content. In this situation, approaches that aggregate spectral signals of pixels belonging to the same parcel to investigate their average behavior, can generate misleading results. In this work, focusing on time series of *NDVI* and *NDWI* spectral indices obtained from Sentinel 2 and Landsat 8 datasets, a cadaster-based landscape tessellation is compared with an image segmentation-based one, with special concerns about rice crops sited in the NW part of Italy. Since tessellation is assumed to drive the local aggregation of spectral signal, differences affecting NDVI and NDWI time series where tested at both spatial and temporal level by computing the above mentioned statistics. Results, obtained for the rice growing season 2016, showed that yearly-averaged local differences were significant (> 0.04 points of spectral index) in about the 23 % and 27 % of segments (respectively for NDVI and NDWI). At the moment authors are not able to give an interpretation key to robustly explain why some areas are more critical than others. The different behaviors of the various parts of the same parcel can rely on many motivations: different crop type, different treatments times, different terrain properties, position of fields in respect of the channel network, etc. Further investigation should be done, whenever the technology transfer occurred, based on local features of the monitored area.

Results about the yearly trend of differences, showed that they suffer from seasonality with a higher incidence in Spring, when rice agronomic phases are more dynamic and, in the meantime, critical for management. $MAE_{x,y}(t)$, in fact, showed that highest differences were concentrated at the beginning of the growing season: mid-April for NDVI, mid-May for NDWI. Moreover they proved to be, averagely in the area, significant, therefore, not negligible.

Consequently, authors retain that, whenever a monitoring service based on time series of spectral indices was developed and launched, cadastral parcels could not be assumed as reference unit to average spectral measures, since the actual agronomic tessellation context (for the study area) is different from the administrative one. From this point of view, image segmentation based on NDVI time series proved to be reliable enough to describe a land division more consistent with the actual field management practices.

Authors are conscious that results cannot be generalized for whatever agricultural context. Nevertheless, the quantification of differences, even if specifically related to the study area, support the general idea that precision farming or administrative controls in agriculture, cannot rely on cadastre basis. Moreover, since the study area is historically devoted to rice cultivation, the results we found in this situation are expected to be optimistic in respect of any other agricultural context: rice fields, here, are known to be homogeneously and extensively managed, reasonably limiting local differences.

Finally, it is worth to remind that, recently, AGEA, the Italian paying agency for agriculture (EU contributions), according to the art. 17, paragraph.2 of the European Union Regulation n. 809/2014, has made mandatory for farmers, starting from the 2018 growing season, the redaction of the so called "*graphic application*": they are, in fact, requested to supply, as much precisely as possible, the georeferenced map of the field they are going to request contribution for, drawing its actual border within a single (or over many) cadastral parcel. Contributions will not anymore be accorded at cadastral parcel level, but in reference of the actual managed field area. In this new legislative context, the suggested approach appears to be more interesting, moving field detection by remote sensing in such a direction consistent with the expected future controls that

AGEA will operate systematically to test consistency of declared areas by farmers, making deductions more reliable.

Disclosure statement: No potential conflict of interest was reported by the authors.

5: References

Barazzetti, L., Cuca, B., & Previtali, M. 2016. "Evaluation of registration accuracy between Sentinel-2 and Landsat 8." In Fourth International Conference on Remote Sensing and Geoinformation of the Environment. International Society for Optics and Photonics.

Borgogno-Mondino, E., Lessio, A., & Gomarasca, M. A. 2016. "A fast operative method for NDVI uncertainty estimation and its role in vegetation analysis." *European Journal of Remote Sensing*, 49(1), 137-156.

Boschetti, M., Nutini, F., Manfron, G., Brivio, P. A., & Nelson, A. 2014 "Comparative analysis of normalised difference spectral indices derived from MODIS for detecting surface water in flooded rice cropping systems." *PloS one*, 9(2).

Comaniciu, D., & Meer, P. 2002. "Mean shift: A robust approach toward feature space analysis." *IEEE Transactions on pattern analysis and machine intelligence*, 24(5), 603-619.

Erden, H., & Öztürk, G. 2015. "Digitization of agricultural parcels". In Agro-Geoinformatics, 2015 Fourth International Conference on, 137-142. IEEE.

Erden, H., Töreyen, G. 2015. "Parcel Based Crop Production Yield Model." In Agro-Geoinformatics, 2015 Fourth International Conference on, pp. 109-112. IEEE.

Forman R.T.T., Godron M. 1986. *Landscape Ecology*. Cambridge University.

Hively, W. D., Lang, M., McCarty, G. W., Keppler, J., Sadeghi, A., & McConnell, L. L. 2009. "Using satellite remote sensing to estimate winter cover crop nutrient uptake efficiency." *Journal of soil and water conservation*, 64(5), 303-313.

Huang, J., Wang, F., Wang, X., Tang, Y., & Wang, R. 2004. "Relationship between narrow band normalized deference vegetation index and rice agronomic variables." *Communications in soil science and plant analysis*, 35(19-20), 2689-2708.

Karantzalos, K., Karmas, A., & Tzotsos, A. 2015. "RemoteAgri: processing online big earth observation data for precision agriculture." *Precision agriculture'15* (pp. 861-873). Wageningen Academic Publishers.

Kliment, T., Bordogna, G., Frigerio, L., Stroppiana, D., Crema, A., Boschetti, M., & Brivio, P. A. 2014. "Supporting a regional agricultural sector with Geo & mainstream ICT-the Case study of space4agri project." *AGRIS on-line Papers in Economics and Informatics*, 6(4), 69.

Lessio, A., Fissore, V., & Borgogno-Mondino, E. 2017. "Preliminary Tests and Results Concerning Integration of Sentinel-2 and Landsat-8 OLI for Crop Monitoring." *Journal of Imaging*, 3(4), 49.

McFeeters S. K. 1996. "The use of the Normalized Difference Water Index (NDWI) in the delineation of open water features", *International journal of remote sensing,* 17(7)

Maclean, J. L., Dawe, D. C., Hardy, B., & Hettel, G. P. 2002. "Rice Almanac: Source Book for the Most Important Economic Activity on Earth." Int. Rice Res. Inst.

McNairn, H., Champagne, C., Shang, J., Holmstrom, D., & Reichert, G. 2009. "Integration of optical and Synthetic Aperture Radar (SAR) imagery for delivering operational annual crop inventories." *ISPRS Journal of Photogrammetry and Remote Sensing*, 64(5), 434-449.

Munyati, C. 2017. “The potential for integrating Sentinel 2 MSI with SPOT 5 HRG and Landsat 8 OLI imagery for monitoring semi-arid savannah woody cover.” *International journal of remote sensing*, 38(17), 4888-4913.

O’ Connell, M., Whitfield, D., & Abuzar, M. 2014. “Satellite remote sensing of vegetation cover and nitrogen status in almond.” In XXIX International Horticultural Congress on Horticulture: Sustaining Lives, Livelihoods and Landscapes (IHC2014): 1130 pp. 559-566.

Reg.EU no. 809/2014 on of the European Parliament and of the Council with regard to the integrated administration and control system, rural development measures and cross compliance.

Rouse Jr, J.W., Haas R. H., Schell J. A., Deering D. W., Harlan J. C. 1974. “Monitoring the vernal advancement of retrogradation of natural vegetation”, Final report. NASA/GSFC.

Willmott, C. J., & Matsuura, K. 2005. “Advantages of the mean absolute error (MAE) over the root mean square error (RMSE) in assessing average model performance.” *Climate research*, *30*(1), 79-82.

Tey, Y. S., & Brindal, M. 2012. “Factors influencing the adoption of precision agricultural technologies: a review for policy implications.” *Precision Agriculture*, 13(6), 713-730.

Tuong, T. P., & Bouman, B. A. M. 2003. “Rice production in water-scarce environments.” *Water productivity in agriculture: Limits and opportunities for improvement*, 1, 13-42.

Zelaya, K., van Vliet, J., & Verburg, P. H. 2016. “Characterization and analysis of farm system changes in the Mar Chiquita basin, Argentina.” *Applied Geography*, 68, 95-103.

Zerbato, C., Rosalen, D. L., Furlani, C. E. A., Deghaid, J., & Voltarelli, M. A. 2016. "Agronomic characteristics associated with the normalized difference vegetation index (NDVI) in the peanut crop." *Australian Journal of Crop Science*, 10(5), 758.

6: Web References

http://agri.istat.it.

https://earthexplorer.usgs.gov.

http://www.enterisi.it.

https://scihub.copernicus.eu.

Figure 1. Study area. White lines = cadastral parcels of rice-cultivated fields. Reference frame is WGS-84 UTM 32N.

Figure 2. Temporal distribution of datasets. The joint use of optical data from different missions (S2 black, L8 grey) improves the acquisition rate especially when datasets are compromised by cloud cover (S2 series from March to July).

Figure 3. Cadaster-based Vs segmentation-based tessellation of rice fields. A: NDVI original image (S2, April 2016); B: Cadaster-based tessellation scheme (cadastral vector map); C: segmentation-based tessellation scheme as generated by OTB; D: at-field level averaging of NDVI (April 2016)based on cadastral parcels; E: at-field level averaging of NDVI (S2, April 2016) based on segmented polygons.

Figure 4. Cumulative frequency distribution of the number of segments per parcel (totally o partially included). The percentage is referred to the total number of cadastral parcels.

Figure 5. Cumulative frequency distributions of Area (left) and SI (right) values computed for the two compared tessellation schemes.

Figure 6. Effects of different tessellation schemes in respect of the local temporal profiles of both NDVI and NDWI. Red line = average spectral index profile of the whole parcel. Segm 1,2,3,4 are the average spectral index profiles of respectively sub-parcels 1,2,3,4. Left: NDVI profiles; Right: NDWI profiles.

Figure 7. Example subsets of MAE maps of NDVI (A) and NDWI (B). Maps are useful to interpret where the most significant differences are located, when monitoring rice fields through a cadaster- or segments-based approach based on remote sensing techniques.

Figure 8. Cumulative frequency distribution functions of NDVI and NDWI MAE maps (count is given considering the number of segments). Significant differences are, precautionary, those higher than 0.04 (vertical line).

Figure 9. MAE(t) temporal profiles of NDVI (left) and NDWI (right). Red line = MAE(t), black triangles = maximum differences at the single date, black squares = minimum differences at the single date. Graphs are useful to interpret if spectral differences are somehow time-dependent, i.e. if and how agronomic phases can heavily be conditioned by the different type of NDVI/NDWI averaging tessellation scheme.

Table 1. Technical features of L8 and S2 datasets.

L8			**S2**					
Temporal resolution: 16 Days			**Temporal resolution: 5 Days**					
Bands	**GSD (m)**	**Wavelength (µm)**	**Bands**	**GSD (m)**	**Wavelength (µm)**	**Bands**	**GSD (m)**	**Wavelength (µm)**
Band 1	30	0.433-0.453	*Band 1*	60	0.423-0.463	*Band 8*	10	0.727-0.957
Band 2	30	0.450-0.515	*Band 2*	10	0.425-0.555	*Band 8a*	20	0.845-0.885
Band 3	30	0.525-0.600	*Band 3*	10	0.525-0.595	*Band 9*	60	0.925-0.965
Band 4	30	0.630-0.680	*Band 4*	10	0.635-0.695	*Band 10*	60	1.350-1.410
Band 5	30	0.845-0.885	*Band 5*	20	0.690-0.720	*Band 11*	20	1.520-1.700
Band 6	30	1.560-1.660	*Band 6*	20	0.725-0.755	*Band 12*	20	2.010-2.370
Band 7	30	2.100-2.300	*Band 7*	20	0.760-0.803			
Radiometric resolution: 16 bit			*Radiometric resolution: 12 bit*					

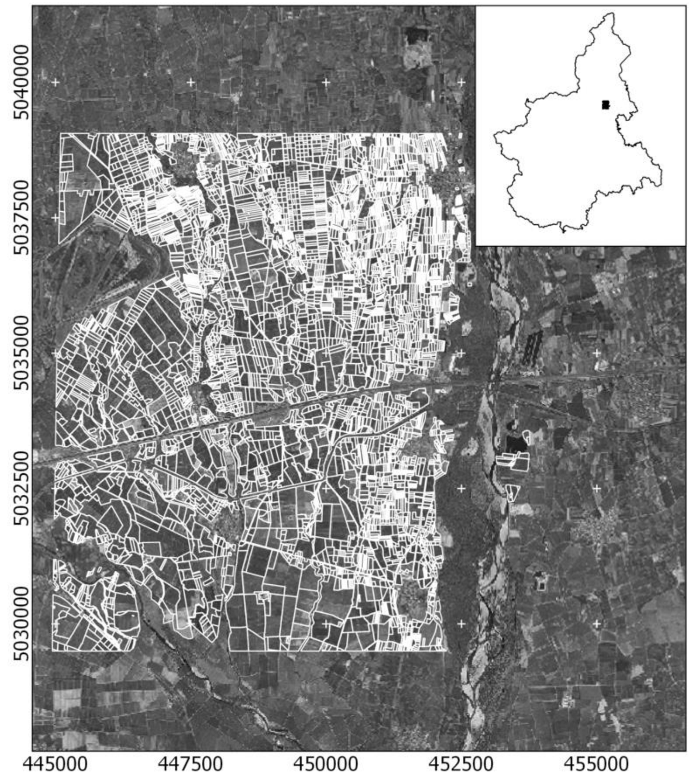

Figure 1

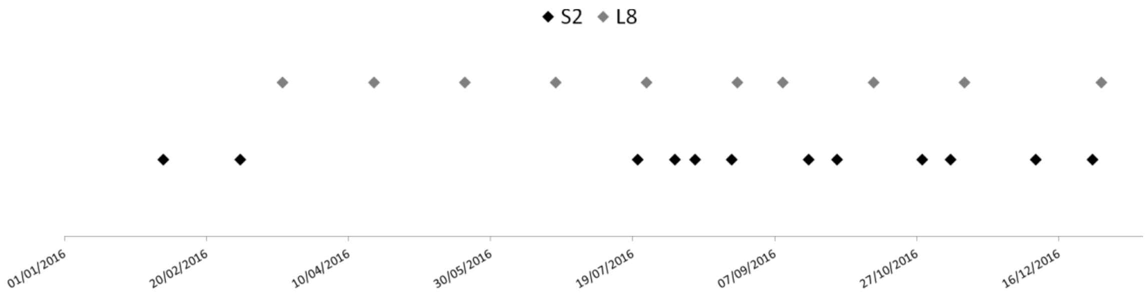

Figure 2

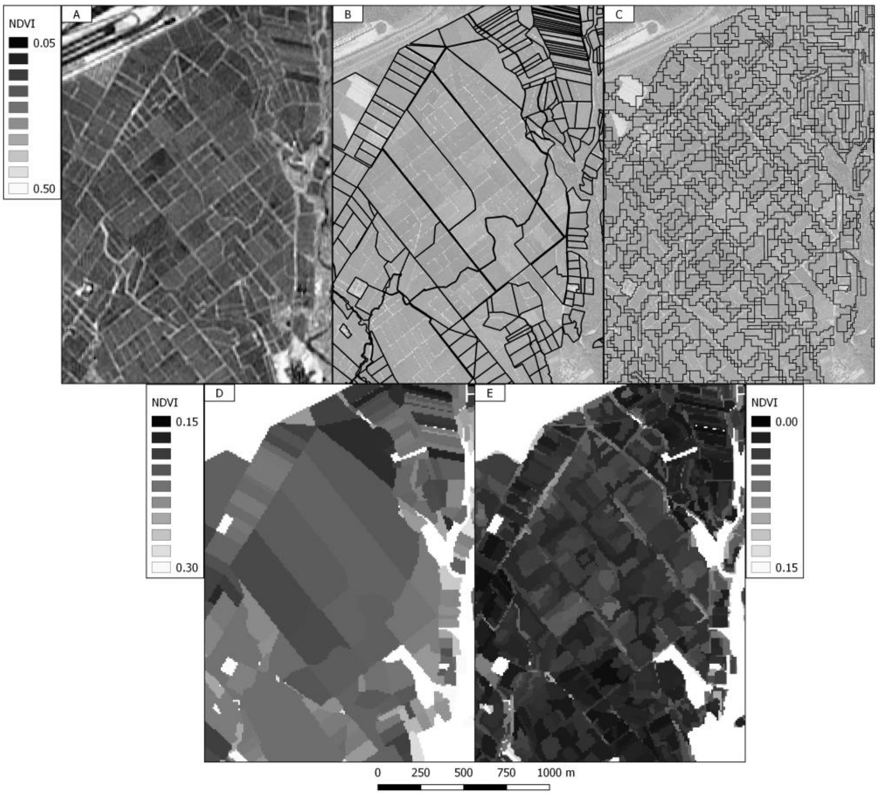

Figure 3

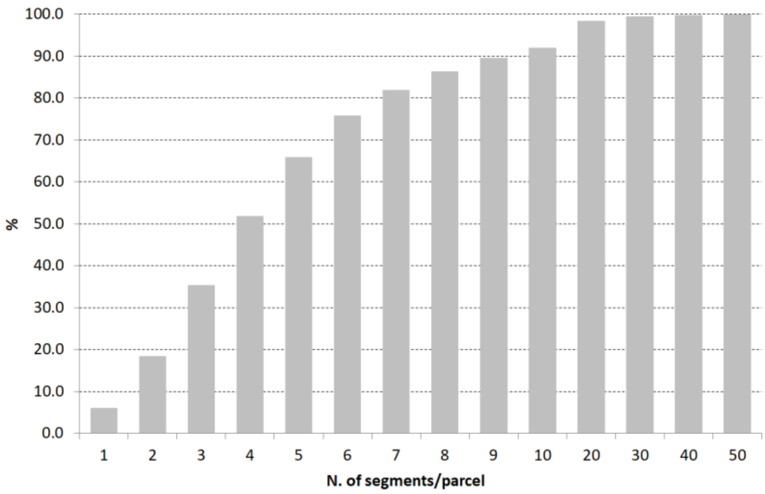

Figure 4 (new addition)

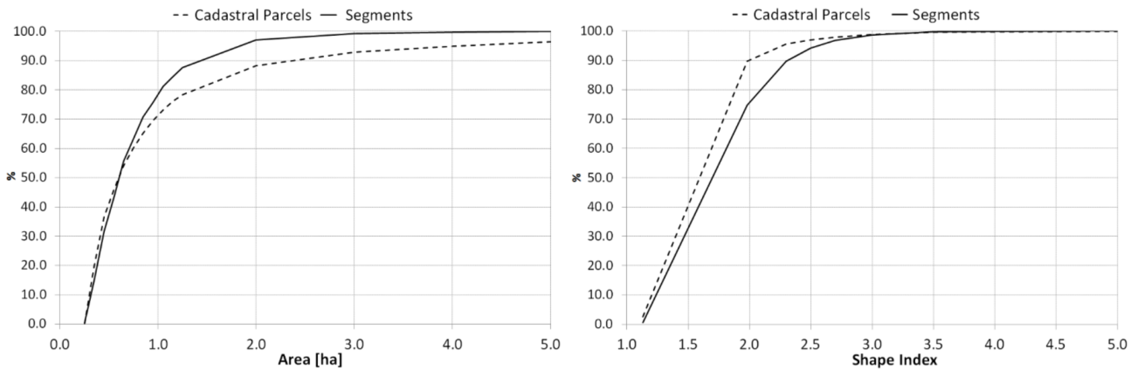

Figure 5

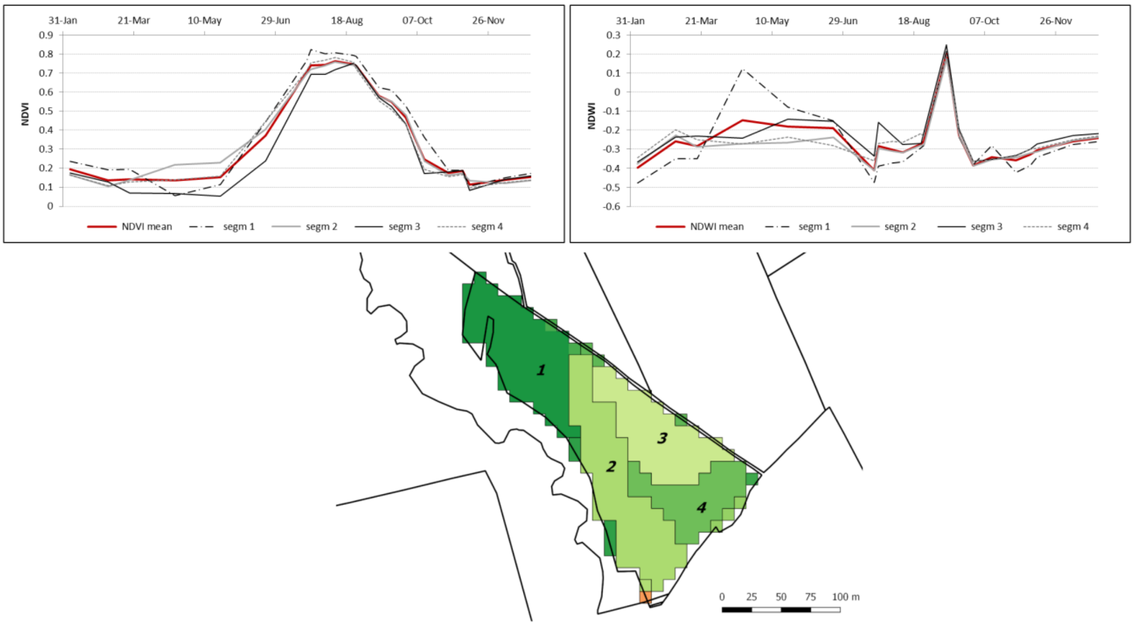

Figure 6

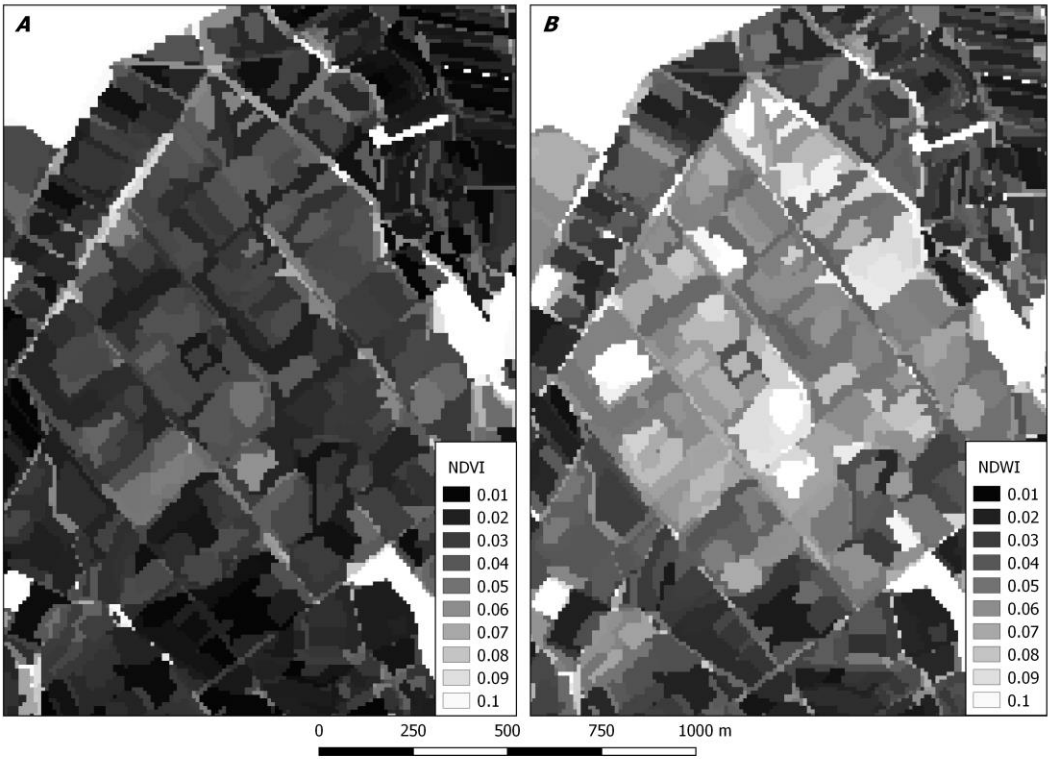

Figure 7

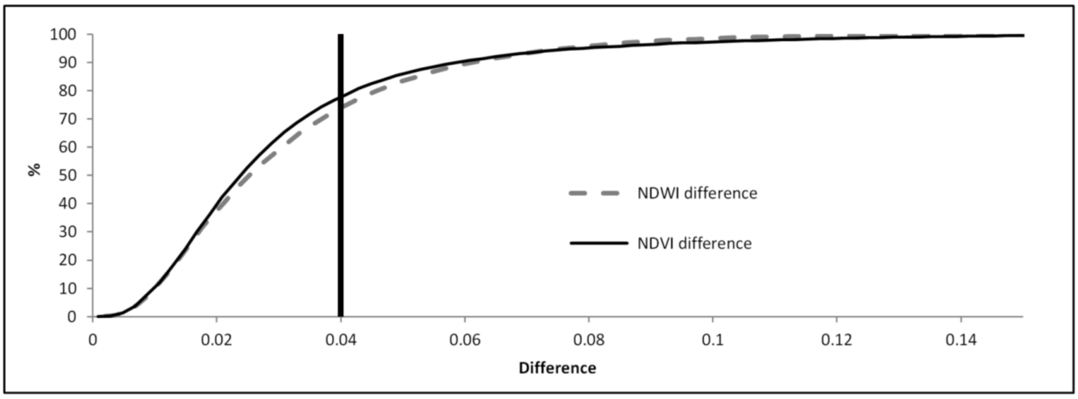

Figure 8 (Changed – ex fig. 7)

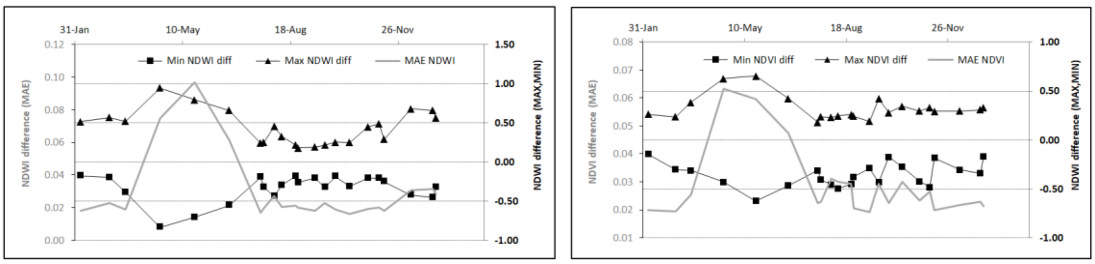

Figure 9 (changed – ex fig.8)